

Multifocus Structure of a Light Beam in a Nonlinear Medium

A. L. DYSHKO, V. N. LUGOVOI, AND A. M. PROKHOROV

P. N. Lebedev Physics Institute, USSR Academy of Sciences

Submitted July 8, 1971

Zh. Eksp. Teor. Fiz. **61**, 2305-2318, (December, 1972)

The time-stationary multifocus structure of a light beam in a medium with a Kerr type of nonlinearity is considered by taking into account various types of nonlinear absorption in the medium. It is shown that under typical conditions the finite sizes of the focal regions are determined by nonlinear absorption in the medium. The dependence of these sizes and of the maximal energy density in the focal regions on the initial beam power and the nonlinear absorption coefficients is investigated.

INTRODUCTION

THE propagation of intense light beams in media with nonlinearities of the Kerr type has recently attracted considerable interest (see, for example, [1-7]). In [1], on the basis of a numerical solution of the corresponding problem, it was shown that the propagation of a light beam that is stationary in time with supercritical power in the medium under consideration can cause the beam to "collapse" at a definite point in the medium. An analogous conclusion was derived in [3]. The picture of beam propagation beyond the collapse point was not, however, considered in [1,3]. This picture was considered in [2], where it was established that a multifocus light-beam structure is produced beyond the collapse point. It became clear simultaneously that the capture of the beam into a regime of self-consistent waveguide propagation previously expected under the conditions in question [8] does not take place. Inasmuch as the nonlinear absorption of the different modes that arise in real media was not taken into account explicitly in [2], the energy density at the focal point in the so-called parabolic approximation (see, for example, [1-3]) turns out to be infinitely large. By the same token, only the picture of formation of the multifocus structure of the beam was determined in [2], and the arrangement of the foci along the beam axis was obtained, but the structure of the focal regions and the dependence of their parameters on factors limiting the energy density in them were not considered. The present article is devoted to these questions.

1. FORMULATION OF PROBLEM

Before we proceed to a solution of concrete problems, let us discuss a number of factors that can limit the energy density at the foci. It must be noted here immediately that, following publication of [2], many authors (see [5-7]) carried out, on the basis of the parabolic approximation, numerical calculations of the propagation of light beams beyond the collapse point (which is the center of the first focus), with allowance for "saturation" of the current nonlinearity. The dependence of the refractive index n on the complex amplitude E of the oscillations of the electric field was written down, for example, in the form

$$n = n_0 + \frac{1/2 n_0 n_2 |E|^2}{1 + |E|^2 / |E_s|^2}, \tag{1}$$

where $|E_s|$ is the amplitude of the oscillations of the intensity of the characteristic saturating field. At $|E|^2 \ll |E_s|^2$, the usual expression holds:

$$n = n_0 (1 + 1/2 n_2 |E|^2), \tag{2}$$

and leads to an infinite energy density at the focal points. At $|E|^2 \gtrsim |E_s|^2$, however, an important role is assumed by the factor that takes saturation into account. Because of this factor, the energy density at the foci ($|E_f|^2$) turns out to be finite, and at the same time satisfies the inequality $|E_f|^2 > |E_s|^2$ (see, for example, [5,6]). This inequality means that on approaching the focus, the growth of the intensity on the beam axis stops only when the refractive index deviates noticeably from a quadratic function of the field. If it is now recognized that, in accord with [2], the power "flowing into" each focus is $P_f \approx P_{cr}^{(1)}$, where

$$P_f^{(1)} = c N_1^2 n_0 / 8 n_2 k^2 \tag{3}$$

($N_1 \approx 2$, $k = 2\pi/\lambda$, $\lambda = 2\pi c/\omega n_0$ is the wavelength in the medium, and ω is the frequency of the field oscillations in the beam), and if we also take into account the usual relation $|E_s|^2 \sim 1/n_2$ (see, for example, [9]), then we obtain immediately $d_f < \lambda/2$, where $d_f = (32 P_f \ln 2 / c n_0 |E_f|^2)^{1/2}$ is the diameter of the focal region, i.e., the parabolic approximation no longer holds in the focal region. Therefore to describe the propagation of a beam with supercritical power in the medium under consideration (with allowance for only the saturation of the nonlinearity), it is necessary to use Maxwell's equations directly without going over to the parabolic approximation.

If we assume now that the finite value of the focal-region diameter is determined precisely within the framework of Maxwell's equation (i.e., that $d_f \sim \lambda$), then for typical media (i.e., media with $n_2 \sim 10^{-11} - 10^{-13}$ cgs esu) we obtain, with allowance for (3), the intensity I_f at the center of the focal region, namely $I_f \sim 10^{12} - 10^{14}$ W/cm². At such intensities, and in most cases at much lower intensities, essentially nonlinear absorption of light can set in in the medium (for example, multiphoton absorption, absorption due to energy transfer into the stimulated scattering components, absorption connected with breakdown of the media, etc.). The appearance of nonlinear absorption of this type in regions of a beam with intensity on the order of $10^{10} - 10^{11}$ W/cm² was recorded in many experiments (see, for example, [10-15]). This means that nonlinear absorption may be the main

factor limiting the energy density in the focal regions, (as was noted earlier in^[4]). In the latter case, the diameters of the focal regions will be much larger than the wavelength λ , which also agrees with the experimental results.

Under the indicated conditions, to describe the propagation of the light beams in the medium one can use the parabolic approximation and at the same time the saturation of the Kerr nonlinearity is automatically negligibly small. Therefore the dependence of the real part of the refractive index of the medium on the light intensity can be taken in the form (2). At the same time, account must be taken of the intensity-dependent imaginary part of the refractive index, due to nonlinear absorption in the medium. We shall consider in detail below, as factors limiting the energy density in the focal regions, three types of nonlinear absorption:

1) three-photon absorption, 2) absorption due to energy transfer into the first Stokes component of stimulated Raman scattering (SRS), and 3) two-photon absorption.

2. MULTIFOCUS STRUCTURE OF LIGHT BEAM WITH ALLOWANCE OF THREE-PHOTON ABSORPTION IN THE MEDIUM

In this section we consider the propagation of an intense monochromatic light beam of frequency ω in a medium with a complex refractive index

$$n = n_0 + 1/2 n_2 |E|^2 + i m_4 |E|^4, \quad (4)$$

where n_2 and m_4 are real coefficients; the imaginary part of this expression describes three-photon absorption in the medium. We shall assume that a parallel axially-symmetrical beam is incident on a half-space $z \geq 0$ filled with a medium having a refractive index (4) normal to the boundary $z = 0$ (the refractive index of the medium at $z < 0$ is assumed to be n_0). The equation for the complex amplitude E in cylindrical coordinates and in the parabolic approximation assumes at $z \geq 0$ the form

$$\frac{\partial^2 E}{\partial r^2} + \frac{1}{r} \frac{\partial E}{\partial r} + 2ik \frac{\partial E}{\partial z} + k^2 (n_2 |E|^2 + i m_4 |E|^4) E = 0 \quad (5)$$

(the values of the electric field intensity \mathcal{E} are connected with the complex amplitude E by the relation

$$\mathcal{E} = (1/2) E \exp(ikz - i\omega t) + \text{c.c.}).$$

We begin the solution of our problem with the case of a Gaussian initial intensity distribution, i.e., we put

$$E|_{z=0} = E_0 \exp\{-r^2 / 2a^2\}. \quad (6)$$

We then change over to the dimensionless variable $X = E/E_0$ which, according to (5) and (6), satisfies the equation

$$\frac{\partial^2 X}{\partial r_1^2} + \frac{1}{r} \frac{\partial X}{\partial r_1} + 2iN \frac{\partial X}{\partial z_1} + (N^2 |X|^2 + i\mu_4 |X|^4) X = 0 \quad (7)$$

with boundary condition

$$X|_{z_1=0} = \exp\{-1/2 r_1^2\} \quad (8)$$

where $r_1 = r/a$, $z_1 = z/l_X$, $l_X = a/\sqrt{n_2 E_0^2}$, $N = E_0/E_{CR}$, $E_{CR} = 1/\sqrt{n_2 (ka)^2}$, and $\mu_4 = m_4 E_0^2 N^2 / n_2$. Equation (7) with boundary condition (8) was solved numerically with a BESM-6 computer. We used an implicit difference scheme analogous to that employed in^[2] (the convergence of the solution of the corresponding difference

equation to the solution of (7) can be proved).

The values of the parameter N were specified in the interval from 2 to 10, corresponding to an approximate variation of the incident-beam power from $P_{CR}^{(1)}$ to $27P_{CR}^{(1)}$; the values of the parameter μ_4 were specified in the interval $10^{-3} < \mu_4 < 0.2$. For different r_1 and z_1 we derived the values of $|X|^2$, and also the ratio of the beam power P at the section z_1 to the power P_0 of the incident beam

$$\frac{P}{P_0} = 2 \int_0^\infty r_1 |X|^2 dr_1.$$

It was established as a result that the structure of the solution coincides with that described in^[2], namely, a finite series of foci are produced on the beam axis as a result of successive focusing of the different annular zones of this beam.

The process of formation of a multifocus beam structure can be easily understood by tracing the evolution of the solution at sufficiently small values of μ_4 and by continuously increasing the parameter N , starting with the value $N_1 \approx 2$, at which the first focus occurs. The power that flows into this focus is close to the critical power $P_{CR}^{(1)}$ (see (3)). With increasing N (i.e., with increasing initial power P_0), the energy flux into the produced focus is not increased, and the excess part of the energy flux goes past the focus in question, so that an autonomous beam is produced far beyond the focus (the energy flowing through the focus goes off from the region of the last beam in the form of an annular wave that diverges rapidly from the focus). So long as the power of the produced beam remains smaller than $P_{CR}^{(1)}$, this beam, in turn, simply diverges without any essential singularities occurring in it. Once its power exceeds a value close to $P_{CR}^{(1)}$ (which corresponds for the parameter N to an excess over a certain value $N_2 > N_1$ and for the initial power to an excess over the value $P_{CR}^{(2)} > P_{CR}^{(1)}$), the next focus is produced in the beam in question, which has passed beyond the first focus. With further increase of the initial power P_0 , the energy fluxes flowing into the first and second foci accordingly do not increase, and the excess part of the energy flux passes beyond both foci, so that an autonomous beam is again produced beyond them. A third, fourth, fifth, etc. focus is subsequently produced in similar fashion whenever the parameter N exceeds a certain succeeding value $N_3 < N_4 < N_5 \dots$ (or the power P_0 exceeds the values $P_{CR}^{(3)} < P_{CR}^{(4)} < P_{CR}^{(5)} \dots$). We note also that after they are produced, all foci approach one another with increasing N , and approach simultaneously the boundary $z = 0$. For large N , the distances between neighboring foci turn out to be much smaller than the distance from the boundary $z = 0$ to the first of the foci. The described structure of the beam is illustrated schematically in Fig. 1.

For a more detailed representation of the character of the solution and the structure of the focal regions, Fig. 2 shows by way of an example the dependences of the quantity $|X|^2$ and of the ratio P/P_0 on z_1 at $N = 6$ and $\mu_4 = 0.05$. The three lower plots in this figure determine the function $|X|^2$ of z_1 on the beam axis (i.e., at $r_1 = 0$) and on two cylinders near the axis ($r_1 = 1/12$ and $r_1 = 1/6$) in the range of z_1 from 0.8 to 1.9 (the first three foci lie in this interval). For convenience, the indicated plots are drawn in different scales (the scale

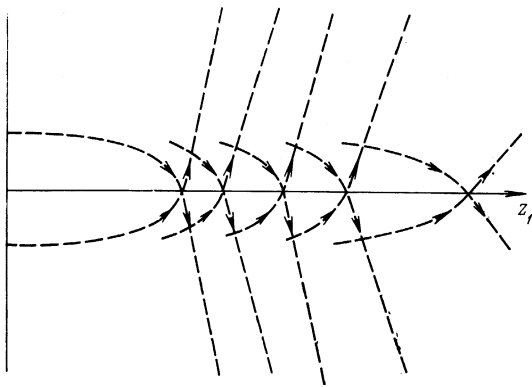


FIG. 1

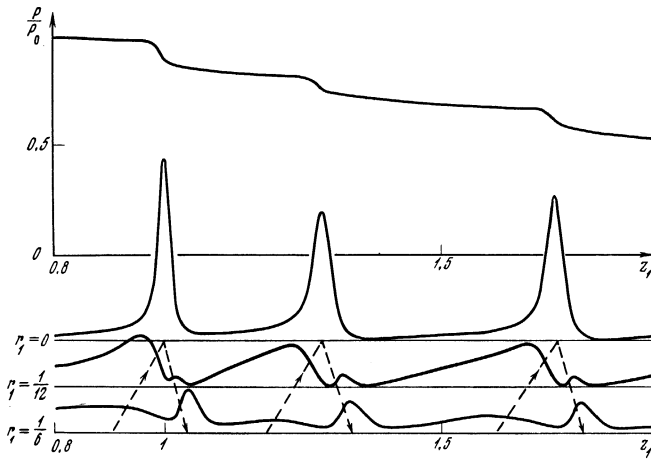


FIG. 2

increases with increasing r_1). The upper plot determines the dependence of the relative beam power P/P_0 on z_1 in the same interval of z_1 .

We see that the dependence of $|X|^2$ on z_1 at $r_1 = 0$ has three sharp peaks corresponding to three focal regions on the beam axis. We see also that the different focal regions have similar structures, a characteristic feature of which is that the dependence of this quantity on z_1 is asymmetrical with respect to the points of the maxima of $|X|^2$ (the rear slope of the corresponding curves is steeper than the front slope). The plots of $|X|^2$ against z_1 for $r_1 = 1/12$ and $r_1 = 1/6$ reflect the process of focus formation and the emergence of the indicated annular waves from the foci (this process is denoted schematically by dashed lines in analogy with Fig. 1). As to the transverse structure of the focal regions themselves (which is determined by the dependence of $|X|^2$ on r_1 at the sections $z_1 = z_{f1}, z_{f2}, z_{f3}, \dots$, where z_{fm} is the point of maximum of $|X|^2$ in the m -th focal region), the corresponding curves corresponding to the first foci under consideration are shown in Fig. 3. We see that the transverse structures of the different focal regions are also similar to one another. This similarity becomes understandable if it is recalled that all the foci are produced by the same mechanism.

An analysis of the solution obtained for large distances from the beam axis ($r_1 \gtrsim 1$) also shows that the annular waves diverging from the different foci (which interfere in general with the wave traveling past the

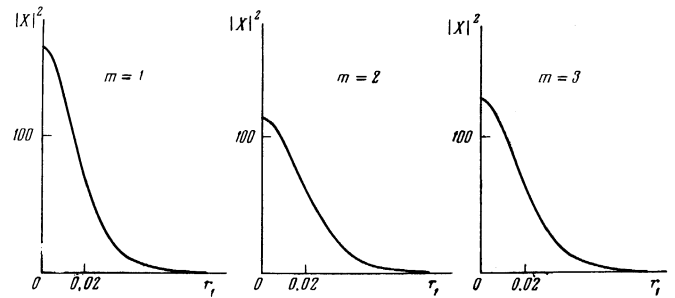


FIG. 3

foci lying ahead of the section z_1 under consideration) produce in the region $r_1 \gtrsim 1$ a complicated annular structure characterized by a series of maxima and minima of the quantity $|X|^2$ as a function of r_1 . The indicated annular structure appears beyond the first focus (i.e., at $z_1 > z_{f1}$). The surface bounding it is well approximated by the surface of a cone with a vertex angle determined by the angle of emergence of the wave from the first focus.

Let us examine now the plot of the relative beam power P/P_0 against z_1 , shown in Fig. 2. We see that the passage of the beam through each focus is accompanied by a decrease of its power P by an amount on the order of $P_{cr}^{(1)}$ (in the case $N = 6$ under consideration we have $P_{cr}^{(1)}/P_0 \approx 0.1$). This decrease of the power is obviously due to the absorption of an appreciable fraction of the electromagnetic energy flowing into the focal region. It is therefore clear that the energy flux P_{fm} through the "central" section in this region (i.e., the section $z_1 = z_{fm}$) should amount to only a certain fraction of $P_{cr}^{(1)}$. Strictly speaking, the quantity P_{fm} is determined accurately to the concrete method of cutting off the solution with respect to r_1 beyond the limits of the focal region. We shall henceforth denote by $|X_{fm}|^2$ the value of $|X|^2$ at the "center" of the m -th focal region, i.e., at $z_1 = z_{fm}$ we have $r_1 = 0$. By P_{fm} we shall mean, for concreteness, the total energy flux carried by a parallel Gaussian beam, for which the maximum value of $|E|^2$ coincides with $|E_{fm}|^2 = E_0^2 |X_{fm}|^2$, and which has a half-width of the transverse intensity distribution (determined at the level $|E_{fm}|^2/2$) the same as the corresponding half-width a_{fm} of the distribution of $|E|^2 = E_0^2 |X|^2$ with respect to r in the plane $z_1 = z_{fm}$ (it is seen in Fig. 3 that the transverse distribution of the intensity in the focal region at $r_1 \leq a_{fm}/a$ is very close to Gaussian). We thus put

$$P_{fm} = \frac{cn_0 a_{fm}^2 |E_{fm}|^2}{8 \ln 2} = \frac{N^2 |X_{fm}|^2 r_{fm}^2 P_{cr}^{(1)}}{N_i^2 \ln 2}, \quad (9)$$

where $r_{fm} = a_{fm}/a$ and $N_i^2 \ln 2 \approx 2.7$. Calculations of P_{fm} , carried out in the entire considered range of values of N and μ_4 , and also for all numbers of the focal regions, yielded practically the same value, $P_{fm} \approx (2/3) P_{cr}^{(1)}$ (with absolute accuracy $0.025 P_{cr}^{(1)}$).

The dependence of $|X_{fm}|^2$ on the parameter μ_4 for sufficiently small values of this parameter is close to all values of N to inverse proportionality ($|X_{fm}|^2 \sim 1/\mu_4$). For a more accurate representation of the character of this dependence, Fig. 4 shows a plot of the function $|X_{f1}|^2$ against $1/\mu_4$ at $N = 6$.

As to the total number of foci in the beam and their

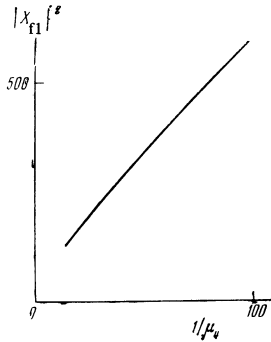


FIG. 4

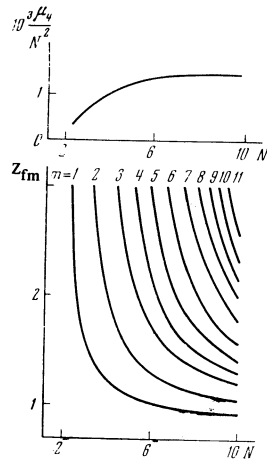


FIG. 5

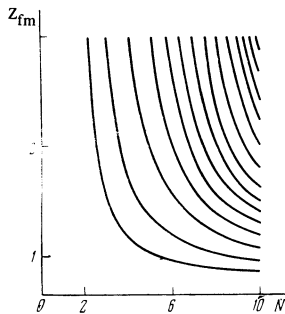


FIG. 6

positions along the z_1 axis, these quantities depend in general on N and μ_4 . At sufficiently small values of μ_4 , however (corresponding to a pronounced multifocus structure in which the values of $|X_{fm}|^2$ are sufficiently large), the positions of the foci z_{fm} depend little on μ_4 and are close to the positions of the foci obtained in^[2] for the case of a vanishingly small absorption of the medium¹⁾. The positions of the foci on the z_1 axis remain strongly dependent in this case only on the parameter N . Figure 5 shows a family of curves determining the dependence of z_{fm} on N . The value of the parameter μ_4 for each N was chosen such as to make $|X_{f1}|^2$ approximately equal to 170, i.e., to make it sufficiently large (a plot of the corresponding values of the ratio μ_4/N^2 against N is also shown in Fig. 5). For comparison, Fig. 6 shows an analogous family of curves obtained in^[2]. We see that these curve families have a similar character and the quantitative differences between them are small (these differences appear mainly for foci with large numbers). The reason for the existence of these differences is the fact that for the assumed values of μ_4 the power absorbed in the intervals between the neighboring focal regions, while small, is nevertheless comparable with the power absorbed in

¹⁾Although the nonlinear absorption in the medium was not taken into account explicitly in [2], the implicit difference scheme employed for the numerical calculations (of first-order accuracy in z_1), as is well known, introduces by itself a certain absorption. If the steps of the difference scheme are made sufficiently small, this absorption becomes vanishingly small in regions not containing singularities of the approximated function, and, generally speaking, the absorption remains finite at the points of discontinuity of this function.

the focal regions themselves (see Fig. 2). With decreasing μ_4 , the power absorbed between neighboring focal regions decreases, and the positions of all the foci approach the positions determined by Fig. 6.

The results shown in Figs. 4 and 5 also make it possible to estimate (at small values of μ_4 and large N) the energy density at the center of the first focus. It is easy to see that at $\mu_4 \lesssim 1/25$ (i.e., $|E_{f1}|^2 \gtrsim 200E_0^2$) and $N \gtrsim 4$ (i.e., $P_0 \gtrsim 4P_{cr}^{(1)}$), the absolute value of this density at the center of the first focus becomes practically independent of the initial beam power, and the corresponding value of $|E_{f1}|^2$ is determined by the formula

$$|E_{f1}|^2 \approx 0.15n_2/m_4, \tag{10}$$

i.e., it is determined only by the constants n_1 and m_4 of the medium. Accordingly, the value of the diameter $d_{f1} = 2a_{f1}$ of the focal region is also determined only by these constants:

$$d_{f1} \approx 1.1\lambda\sqrt{m_4}/n_2. \tag{11}$$

In concluding this section, we note that the considered picture of beam propagation in the medium in question remains completely the same also for the case of beams with other "smooth" initial intensity distributions in the cross section.

3. MULTIFOCUS STRUCTURE OF LIGHT BEAMS WITH ALLOWANCE FOR THE FIRST STOKES SRS COMPONENT

A consistent description of the considered process of light-beam propagation with allowance for the SRS phenomenon in the medium entails, generally speaking, difficulties connected with the need for taking into account the δ -correlated priming sources of the scattered (Stokes) radiation that are distributed in the medium (see [16]). We consider therefore only a model situation, wherein the energy is transferred from the main beam only into one first Stokes component, which, in turn, is initiated by a determined monochromatic "priming" beam incident, like the main beam, from the outside on the boundary $z = 0$ of the medium in question. If the Kerr effect is taken into account for the first Stokes component, then, owing to the proposed coherence of this beam, autonomous focal regions could be produced in the beam. We therefore take the Kerr effect into account for the main beam and do not take it into account with respect to the beam of the first Stokes frequency. Both beams are assumed to be axially symmetrical. In most cases of practical interest, one can also neglect the change of the population of the fundamental vibrational state of the molecules of the medium. We thus arrive at the following system of equations (in the parabolic approximation) for the complex amplitude E , pertaining to the main beam, and the complex amplitude E_{-1} , pertaining to the beam of the first Stokes frequency:

$$\begin{aligned} \frac{\partial^2 E}{\partial r^2} + \frac{1}{r} \frac{\partial E}{\partial r} + 2ik \frac{\partial E}{\partial z} + k^2 \left(n_2 |E|^2 + i \frac{4\pi\Gamma}{n_0^2} |E_{-1}|^2 \right) E &= 0, \\ \frac{\partial^2 E_{-1}}{\partial r^2} + \frac{1}{r} \frac{\partial E_{-1}}{\partial r} + 2ik_{-1} \frac{\partial E_{-1}}{\partial z} - i \frac{4\pi\Gamma}{n_0^2} |E|^2 E_{-1} &= 0. \end{aligned} \tag{12}$$

Here $k_{-1} = 2\pi/\lambda_{-1}$; $\lambda_{-1} = 2\pi c/\omega_{-1}n_0$; $\omega_{-1} = \omega - \omega_0$ is the first Stokes frequency; ω_0 is the frequency of the vibrational transition of the medium with which the SRS proc-

ess is connected; $\Gamma = 3\lambda^{-4}N_0Q_0/2^8\pi^5\hbar\Delta\omega$; Q_0 and $\Delta\omega$ are respectively the cross section and the width of the spectral line of the ordinary (spontaneous) Raman scattering; N_0 is the density of the molecules of the medium; the values of the electric field intensity \mathcal{E}_{-1} are connected with the complex amplitude E_{-1} by the relation $\mathcal{E}_{-1} = \frac{1}{2}E_{-1}\exp(ik_{-1}z - i\omega_{-1}t) + c.c.$ The term with the coefficient Γ in the first equation describes the positive absorption introduced into the main beam by the field of the first Stokes component. The term with the same coefficient in the second equation describes the negative absorption introduced into the Stokes-frequency beam by the field of the main beam.

The system (12) will be considered below under the conditions

$$E|_{z=0} = E_0 \exp\{-r^2/2a^2\}, \quad E_{-1}|_{z=0} = E_{-10} \exp\{-r^2/2a^2\}, \quad (13)$$

which signify a Gaussian initial distribution of the intensities of both beams with identical radius of this distribution and a plane phase front of these beams in the initial section. Introducing the dimensionless quantities the preceding section and also the notation

$$H = ka\sqrt{\frac{4\pi\Gamma}{n_0^2}E_0^2}, \quad Y = \frac{E_{-1}}{E_0}, \quad \xi = \frac{k_{-1}}{k} = \frac{\omega_{-1}}{\omega},$$

we arrive at the following system of equations for the dimensionless quantities X and Y :

$$\begin{aligned} \frac{\partial^2 X}{\partial r_1^2} + \frac{1}{r_1} \frac{\partial X}{\partial r_1} + 2iN \frac{\partial X}{\partial z_1} + (N^2|X|^2 + iH^2|Y|^2)X &= 0, \\ \frac{\partial^2 Y}{\partial r_1^2} + \frac{1}{r_1} \frac{\partial Y}{\partial r_1} + 2iN\xi \frac{\partial Y}{\partial z_1} - i\xi^2 H^2|X|^2 Y &= 0 \end{aligned} \quad (14)$$

with the boundary condition

$$X|_{z_1=0} = \exp\{-1/2r_1^2\}, \quad Y|_{z_1=0} = \alpha \exp\{-1/2r_1^2\}, \quad (15)$$

where $\alpha = E_{-10}/E_0$ is the ratio of the initial field intensity on the axis of the priming beam to the initial intensity of the field on the axis of the main beam. The quantity α in all the foregoing calculations was assumed equal to 10^{-4} , corresponding to an intensity ratio 10^{-8} ; the value of ξ determined by the ratio of the first Stokes frequency to the frequency of the main beam was assumed to be 0.9; the values of N and H were specified independently of each other in the interval from 4 to 10.

As a result of the performed series of calculations it was established that for each value of N there exists a value $H = H_{cr}(N)$ such that at $H < H_{cr}$ the solution is a multifocus structure in which the positions of the foci coincide well with the positions of the foci determined by Fig. 6, and the energy densities at the center of the foci turn out to be infinitely large. At $H > H_{cr}$ the solution is completely defined (bounded) in the entire region $z_1 \geq 0$. In the latter case, if H exceeds H_{cr} only slightly, then the obtained solution also represents a multifocus structure, in which the positions of the first few foci differ only little from the positions of the corresponding foci on Fig. 6. The values of the energy density $|X_{fm}|^2$ in the focal regions at such values of H are determined by the following character of the interaction of the main and Stokes beams; in the layer of the medium from the initial plane $z_1 = 0$ to the first focal region, the intensity of the Stokes component ($|Y|^2$) increases rapidly (exponentially because of the gain), but nevertheless, owing to the small initial values, it remains much smaller

than the intensity ($|X|^2$) of the main component. By the same token, the presence of SRS does not prevent the formation of a focal region, which becomes manifest in the form of a sharp maximum of the quantity $|X|^2$ as a function of z_1 at $r_1 = 0$. In focal region itself, the Stokes SRS component turns out to be comparable in intensity with the main component. Inasmuch as in this case the width of the transverse distribution of the intensity $|Y|^2$ of the Stokes component turns out to be very small (as does also the width of the transverse distribution of the main component $|X|^2$), the intensity of the Stokes component on the axis decreases substantially beyond the first focal region, owing to the diffraction divergence, and by the same token, the formation of the next focal region becomes possible. However, the indicated diffraction decrease of the Stokes-component intensity beyond the first focus is much slower than its growth (which is exponential) in the region ahead of the first focus. Therefore at the start of formation of the second focal region, the Stokes component turns out to be much more intense and limits the energy density $|X|^2$ in this region more effectively. Accordingly we obtain $|X_{f_2}|^2 \ll |X_{f_1}|^2$. The influence of the first Stokes component becomes manifest to a still greater degree in the formation of the third focal region, as a result of which $|X_{f_3}|^2 < |X_{f_2}|^2$. With further increase of z_1 , the energy flux in the Stokes beam may turn out to be so large that further formation of focal regions becomes impossible, owing to the excessively large absorption in the main beam, when the tendency for the intensity to increase on the axis upon formation of the focus is completely suppressed by the absorption. Therefore the total number of foci will in general be smaller than in the case when there is no Stokes beam.

Figure 7 shows by way of an example plots of the function $|X|^2$ against z_1 at $N = 6$, $H = 1.04H_{cr}$ ($H_{cr} \approx 7$). The three continuous curves in this figure determine the function $|X|^2$ of z_1 respectively on the beam axis (i.e., at $r_1 = 0$) and on two cylinders $r_1 = 1/12$ and $r_1 = 1/6$ in the z_1 interval from 0.8 to 1.9. Each of the indicated plots is drawn in the same scale as the corresponding plot in Fig. 2. The dashed lines in Fig. 7 denote schematically the formation of the foci and the emergence of annular waves from them (in the example considered here, the total number of foci in the main beam is equal

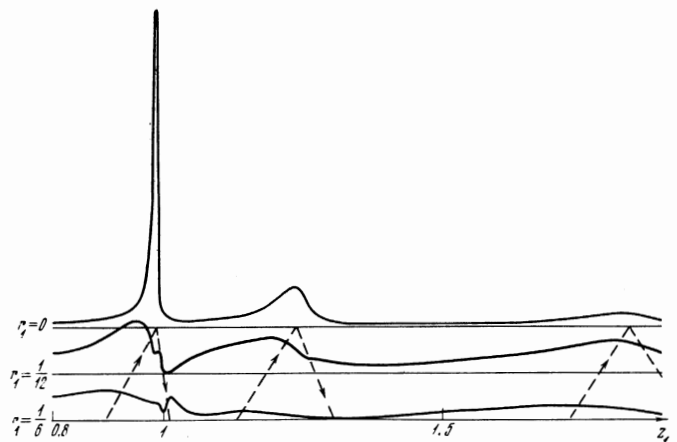


FIG. 7

to three, and all three foci lie in the given interval of z_1). It is interesting to note that the interference between the annular wave emerging from the second focus and the wave traveling past this focus at $r_1 = 1/6$ and $z_1 \approx 1.132$ leads in the present case to a deep trough in the relief of the intensity $|X|^2$ (see Fig. 7).

We note also that the power P_{fm} flowing through the central cross section of the m -th focal region is practically the same (with absolute accuracy $0.01P_{cr}^{(1)}$) in our example for all three focal regions namely $P_{fm} \approx 0.7P_{cr}^{(1)}$. Taking this into account and starting from the values of $|X_{fm}|^2$ determined by the plot of Fig. 7, we can easily determine also the transverse dimensions of the corresponding focal regions. We see that these dimensions increase rapidly with increasing number of the focus, owing to the rapid decrease of $|X_{fm}|^2$ with increasing m . For this reason, when a similar picture is experimentally observed, it is possible to register only one (the first) focus, if the sensitivity of the receiving apparatus is insufficient for the registration of regions with much lower energy density.

4. MULTIFOCUS STRUCTURE OF LIGHT BEAM WITH ALLOWANCE FOR TWO-PHOTON ABSORPTION IN THE MEDIUM

If the main mode of absorption in the medium is two-photon absorption, then the imaginary part of the complex refractive index n of this medium is proportional to $|E|^2$:

$$n = n_0 + \frac{1}{2}n_0(n_2|E|^2 + im_2|E|^2). \tag{16}$$

Here n_2 and m_2 are real coefficients. The propagation of an axially symmetrical light beam in the medium under consideration with boundary condition (6) is described in the parabolic approximation by the following equation for the quantity $X = E/E_0$:

$$\frac{\partial^2 X}{\partial r_1^2} + \frac{1}{r_1} \frac{\partial X}{\partial r_1} + 2iN \frac{\partial X}{\partial z_1} + (N^2|X|^2 + i\mu_2|X|^2)X = 0 \tag{17}$$

with boundary condition (8). We have introduced here the notation from Sec. 2, and also $\mu_2 = m_2N^2/n_2$.

Equation (17) was solved at different values of N and μ_2 . As a result of the performed series of calculations, it was established that in the (N, μ_2) plane there exists a curve $\mu_2 = \mu_{2cr}(N)$ such that when $\mu_2 < \mu_{2cr}$ the solution is a multifocus structure with infinitely large values of the energy density at the centers of the foci (similar to the case $H < H_{cr}$ in the preceding section); when $\mu_2 > \mu_{2cr}$, the solution is perfectly defined in the region $z_1 \geq 0$. In the latter case, if the value of μ_2 does not greatly exceed the value of μ_{2cr} (for example $\mu_{2cr} < \mu_2 < 2\mu_{2cr}$), then the obtained solution is also a multifocus structure. A feature of this structure, however, is the fact that the positions of the foci in it differ greatly from the positions of the foci determined in Fig. 6 for the case of a vanishingly small absorption of the medium. This difference is due to the fact that two-photon absorption is vanishingly small only at sufficiently low values of the coefficient μ_2 , whereas when $\mu_2 > \mu_{2cr}$ this absorption is always finite, i.e., the power absorbed between neighboring focal regions (and in the interval from the initial plane $z_1 = 0$ to the first focal region) will be finite. For the same reason, the total number of foci is also noticeably smaller than in the absence of

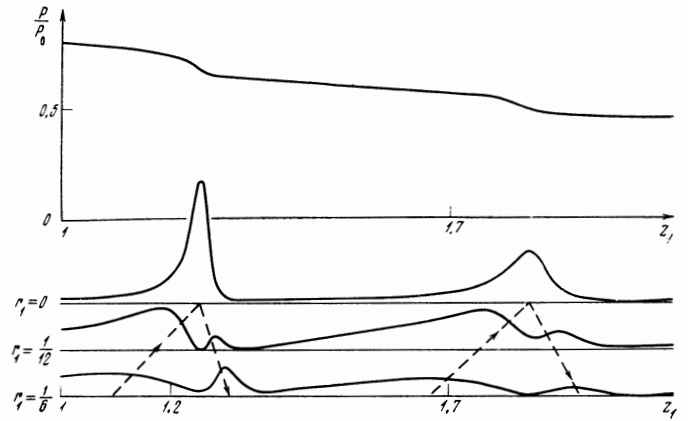


FIG. 8

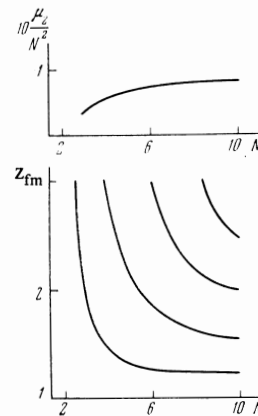


FIG. 9

two-photon absorption in the medium. Nonetheless, the mechanism of formation of the foci themselves and the structure of the beam turn out to be the same as in the case of vanishingly small absorption of the medium.

Figure 8 shows three plots of $|X|^2$ as a function of z_1 for $r_1 = 0, 1/12$, and $1/6$, respectively; $N = 6$ and $\mu_2 = 2.6$ ($\mu_{2cr} < 2.6 < 2\mu_{2cr}$). Each of these plots is drawn in the same scale as the corresponding plot in Fig. 2. The first two foci lie in the interval $1 < z_1 < 2.1$ shown in Fig. 8. Comparing Fig. 2 and Fig. 8, we see that qualitatively, the features of focus formation and of the emergence of annular waves from the foci are the same in the cases of two- and three-photon absorption. The dependence of the relative beam power P/P_0 on z_1 , represented by the upper plot in Fig. 8, also shows that the power absorbed in each focus is on the order of $P_{cr}^{(1)}$. In addition, an appreciable fraction of the beam power is absorbed in the interval between the initial plane $z_1 = 0$ and the first focal region and between neighboring focal planes. Calculation of the power P_{fm} flowing through the central section of the m -th focal region yielded $P_{f1} \approx 0.61 P_{cr}^{(1)}$ and $P_{f2} \approx 0.66 P_{cr}^{(1)}$.

As to the positions of the foci z_{fm} on the z_1 axis, these quantities depend on the parameters N and μ_2 . Figure 9 shows a family of plots of z_{fm} against N for certain selected values of μ_2 . The values of μ_2 were chosen for each N such as to leave the quantity $|X_{f1}|^2$ constant at approximately 110. A plot of the corresponding ratio μ_2/N^2 against N is also shown in Fig. 9. Com-

paring Figs. 5 and 9 (or Figs. 2, 7 and 8) we see that in two-photon absorption the distances between the foci in the multifocus structure can be significantly larger than in other types of nonlinear absorption.

DISCUSSION OF RESULTS

The foregoing results show that propagation of an intense light beam in a large number of material media with nonlinearities of the Kerr type leads to the occurrence of a multifocus structure of this beam. In accordance with^[4], the concrete form of the nonlinear absorption in the medium determines only a number of quantitative characteristics (the values of the energy density in the focal regions, the dimensions of these regions, their number, and their relative placement). At the same time, the qualitative picture of beam propagation turns out to be independent of the types of absorption under consideration.

A multifocus beam structure is certain to arise in those cases when the nonlinear absorption of the medium becomes manifest only in the focal regions and does not exert a direct noticeable influence on the remaining regions of the beam, and without preventing, in particular, the formation of the focal regions themselves. It has been shown in Sec. 2 that this condition is satisfied by three-photon absorption at sufficiently low values of the coefficient m_4 (see (4)). This condition will obviously be satisfied also by four-photon, five-photon, etc. absorption at sufficiently low values of the corresponding coefficients m_6, m_8, \dots . For the case of k -photon absorption ($k \geq 4$), expressions (10) and (11), which determine the energy density and the diameter of the transverse distribution of the intensity in the first focal region, can apparently be generalized as follows:

$$|E_{f1}|^2 \sim \left(\frac{0.15n_2}{m_{2k-2}} \right)^{1/(k-2)} ;$$

$$d_{f1} \sim 0.15\lambda \left[\frac{m_{2k-2}}{(0.15n_2)^{k-1}} \right]^{1/(2k-4)} .$$

The examples of other types of nonlinear absorption considered in Secs. 3 and 4 also show that a multifocus structure of the beam can also arise in the case of large absorption outside the focal regions. In the latter case, the total number of foci and their disposition on the beam axis depend significantly on the power absorbed outside the foci.

It is also of interest to note that it follows formally from expression (11), under the condition $\sqrt{m_4} \lesssim n_2$, that $d_{f1} \lesssim \lambda$. The latter means that this expression cannot be used at $\sqrt{m_4} \lesssim n_2$, since the initially assumed parabolic approximation is no longer valid. If we also disregard other types of nonlinear absorption, then the picture of beam propagation will be described by

Maxwell's equations, within the framework of which there should appear a wave reflected from the collapse point either backward or at large angles to the beam axis. With respect to the wave passing through the collapse point, this reflection will obviously be equivalent to nonlinear absorption (which appears only when the transverse dimension is of the order of λ). One can therefore expect a multifocus structure of the light beam to appear also in the absence of a true nonlinear absorption in the medium.

In conclusion, we call attention to the fact that the foci form a dense chain on the axis at very large supercritical powers of the incident beam. It follows from the investigation reported above that at such powers, and even at the previous small values of the nonlinear absorption coefficient, the neighboring focal regions overlap, i.e., a finite chain of "merged" foci is produced. This chain differs in principle from a waveguide in that no wave propagates in it and in that it does not exist separately from the remainder of the beam. In this chain there occurs a practically continuous absorption (on the z axis) of electromagnetic energy that flows into it from the beam regions off the axis.

¹P. L. Kelley, Phys. Rev. Lett. 15, 1005 (1965).

²A. L. Dyshko, V. N. Lugovoi and A. M. Prokhorov, Zh. Eksp. Teor. Fiz., Pis'ma Red. 6, 655 (1967) [JETP Lett. 6, 146 (1967)].

³V. N. Gol'dberg, V. I. Talanov and R. E. Erm, Izv. MVSSO, Radiofizika 10, 674 (1967).

⁴V. N. Lugovoi and A. M. Prokhorov, Zh. Eksp. Teor. Fiz., Pis'ma Red. 7, 153 (1968) [JETP Lett. 7, 117 (1968)].

⁵J. H. Marburger and E. Dawes, Phys. Rev. Lett. 21, 556 (1968).

⁶E. L. Dawes and J. H. Marburger, Phys. Rev. 179, 862 (1969).

⁷V. E. Zakharov, V. V. Sobolev, and V. S. Synakh, Zh. Eksp. Teor. Fiz. 60, 136 (1971) [Sov. Phys. JETP 33, 77 (1971)].

⁸R. Y. Chiao, E. Garmire, and C. H. Townes, Phys. Rev. Lett. 13, 479 (1964).

⁹R. G. Brewer, J. R. Lifshitz, E. Garmire, R. Y. Chiao, and C. H. Townes, Phys. Rev. 166, 326 (1968).

¹⁰R. G. Brewer and J. R. Lifshitz, Phys. Lett. 23, 79 (1966).

¹¹R. Y. Chiao, M. A. Johnson, S. Krinsky, H. A. Smith, C. H. Townes, and E. Garmire, IEEE J. Quantum Electron. 2, 467 (1966).

¹²R. G. Brewer and C. H. Townes, Phys. Rev. Lett. 18, 196 (1967).

¹³V. V. Korobkin and R. V. Serov, Zh. Eksp. Teor. Fiz., Pis'ma Red. 6, 642 (1967) [JETP Lett. 6, 135 (1967)].

¹⁴V. V. Korobkin, A. M. Prokhorov, R. V. Serov, and M. Ya. Shchelev, Zh. Eksp. Teor. Fiz., Pis'ma Red. 11, 153 (1970) [JETP Lett. 11, 94 (1970)].

¹⁵N. I. Lipatov, A. A. Manenkov, and A. M. Prokhorov, Zh. Eksp. Teor. Fiz., Pis'ma Red. 11, 444 (1970) [JETP Lett. 11, 300 (1970)].

¹⁶V. N. Lugovoi, Vvedenie v teoriyu vyzhdenennogo kombinatsionnogo rasseyaniya (Introduction to the Theory of Stimulated Raman Scattering), Nauka, 1968.